Available online at www.sciencedirect.com

ScienceDirect

Geochimica et Cosmochimica Acta 250 (2019) 34–48

Geochimica et Cosmochimica Acta

www.elsevier.com/locate/gca

Constraining the application of hydrogen isotopic composition of alkenones as a salinity proxy using marine surface sediments

Gabriella M. Weiss [a,*], Stefan Schouten [a,b], Jaap S. Sinninghe Damsté [a,b]
Marcel T.J. van der Meer [a]

[a] Department of Marine Microbiology and Biogeochemistry, NIOZ Royal Netherlands Institute for Sea Research, and Utrecht University, 1790 AB Den Burg, the Netherlands

[b] Department of Earth Sciences, Faculty of Geosciences, Utrecht University, Utrecht, the Netherlands

Received 17 June 2018; accepted in revised form 29 January 2019; Available online 6 February 2019

Abstract

Sea surface salinity is an essential environmental parameter necessary to understand past changes in global climate. However, reconstructing absolute salinity of the surface ocean with high enough accuracy and precision remains a complicated task. Hydrogen isotope ratios of long-chain alkenones (δ^2H_{C37}) have been shown to reflect salinity in culture studies and have been proposed as a tool to reconstruct sea surface salinity in the geologic record. The correlation between δ^2H_{C37} – salinity in culture is prominently caused by the relationship between δ^2H_{H2O} and salinity, as well as the increase in fractionation factor α with increasing salinity. The δ^2H_{C37} – salinity relationship in the natural environment is poorly understood. Here, surface sediments from a variety of environments covering a wide range of salinities were analyzed to constrain the environmental relationship between salinity and hydrogen isotopes of alkenones. δ^2H_{C37} correlates significantly ($r = 0.75$, $p < 0.0001$) with annual mean salinity. Interestingly, the biological hydrogen isotope fractionation (α_{C37}) seems independent of salinity. These findings are different from what has previously been observed in culture experiments, but align with other environmental datasets and suggest that the salinity effect on biological hydrogen isotope fractionation observed in culture is not apparent in sediments. The absence of a correlation between α_{C37} and salinity for marine surface sediments might be best explained by a mixing of multiple alkenone-producing species contributing to the sedimentary alkenone signal that fractionate in distinct ways. Nevertheless, sedimentary δ^2H_{C37} ratios still correlate with salinity and δ^2H_{H2O}, suggesting that δ^2H_{C37} ratios are useful for paleosalinity reconstructions. Our surface sediment calibration presented here can be used when different species contribute to the sedimentary alkenone pool and substantial changes in salinity are expected.

Keywords: Hydrogen isotopes; Alkenones; Surface sediments; Salinity

1. INTRODUCTION

Understanding changes in surface ocean salinity in the past would greatly increase knowledge about ocean circulation and heat transport around the globe with respect to global climate changes. A reliable tool to reconstruct sea surface salinity has long been sought after by the paleoceanographic community. A number of possibilities have been explored, but the reconstruction of sea surface salinity changes can be quite complicated (Rohling, 2007 and references therein). Thus, no direct proxy to reconstruct absolute paleosalinities exists to date. Attempts to understand past salinity changes have employed dinoflagellate (dinocysts) (Wall and Dale, 1968) and diatom assemblages in combination with transfer functions (Fritz et al., 1991; Wilson et al.,

* Corresponding author.
E-mail address: gabriella.weiss@nioz.nl (G.M. Weiss).

https://doi.org/10.1016/j.gca.2019.01.038
0016-7037/© 2019 The Authors. Published by Elsevier Ltd.

1994), but these are qualitative rather than quantitative. Both oxygen and hydrogen isotopes of water have been shown to have a strong quantitative relationship with salinity (Craig and Gordon, 1965). After a correction for calcification temperature using Mg/Ca ratios, oxygen isotope ratios of foraminiferal calcite can be used to reconstruct water oxygen isotope ratios and in turn salinity (e.g. Duplessy et al., 1991; Rohling, 2000). This method is not without issue since temporal changes in the salinity-water isotope ratio relationship occur through time, causing large uncertainties to be associated with these paleosalinity estimates (Rohling, 2007, and references cited therein). Hydrogen isotope ratios can be used to estimate salinity in complement to oxygen isotope ratios since the two are strongly correlated to one another, most commonly evidenced by the global meteoric water line (Craig and Gordon, 1965). Hydrogen isotope ratios of biomarker lipids have been shown to relate to the hydrogen isotope ratios of water, both in culture and natural waters (i.e., lakes), albeit with a large biological fractionation effect (Sachse et al., 2012 and references cited therein). Thus, organic molecules could potentially be valuable proxy carriers for reconstructing the hydrogen isotopic composition of paleo water once the effect of biological fractionation is constrained.

For the marine environment, hydrogen isotope ratios measured on long-chain alkenones have been proposed as a tool to reconstruct changes in salinity (e.g. Schouten et al., 2006; van der Meer et al., 2007; Wolhowe et al., 2009; Leduc et al., 2013; Kasper et al., 2014; Sachs et al., 2016). Long-chain alkenones are produced exclusively by haptophyte algae of the order Isochrysidales (de Leeuw et al., 1980; Volkman et al., 1980). Alkenones are an attractive compound of interest due to their species specificity and the fact that the hydrogen they contain is non-exchangeable. Culture experiments, most prominently with the common modern-day marine alkenone-producing haptophyte, *Emiliania huxleyi*, show a strong linear trend between hydrogen isotope ratios of C_{37} alkenones (δ^2H_{C37}) and salinity (Schouten et al., 2006; Wolhowe et al., 2009; M'Boule et al., 2014; Sachs et al., 2016; Weiss et al., 2017). The relationship between δ^2H_{C37} and salinity has a steeper slope than the δ^2H_{H2O}-salinity relationship showing that biological hydrogen isotope fractionation between alkenones and growth water is decreasing and the fractionation factor α_{C37} is increasing with salinity (Schouten et al., 2006; Wolhowe et al., 2009; M'Boule et al., 2014; Sachs et al., 2016; Weiss et al., 2017). As a result, the correlation between δ^2H_{C37} ratios and salinity in culture studies is the effect of both the hydrogen isotopic composition of the water and biological hydrogen isotope fractionation. Previous culture experiments have focused on the effects of different environmental parameters on α_{C37} values (Schouten et al., 2006; Wolhowe et al., 2009; Chivall et al., 2014; M'Boule et al., 2014; Sachs and Kawka, 2015; Sachs et al., 2016; Weiss et al., 2017). Several variables have been highlighted that appear to have an influence on α_{C37} values, e.g., salinity, growth rate, growth phase, light intensity, and species (Schouten et al., 2006; Wolhowe et al., 2009; Chivall et al., 2014; M'Boule et al., 2014; van der Meer et al., 2015). Alkalinity and temperature have been shown to have a negligible effect on α_{C37} values (Schouten et al., 2006; Weiss et al., 2017). However, the influence of these parameters on α_{C37} values, and therefore δ^2H_{C37} ratios, in the natural environment is poorly understood.

Despite this, there have been several paleo reconstructions of salinity using δ^2H_{C37} ratios. These reconstructions all show reasonable relative changes in salinity suggesting that δ^2H_{C37} ratios are a suitable paleoceanographic tool (van der Meer et al., 2007; Pahnke et al., 2007; Leduc et al., 2013; Kasper et al., 2014; Petrick et al., 2015; Simon et al., 2015). Nevertheless, an environmental calibration for the δ^2H_{C37}-salinity relationship is necessary to bridge the gap between culture studies and paleo reconstructions. δ^2H_{C37} ratios from surface sediments in the Chesapeake Bay Estuary, USA, were analyzed for hydrogen isotope ratios of alkenones (Schwab and Sachs, 2011). A positive linear correlation between $\delta^2H_{alkenone}$ and salinity is observed, but there is no relationship between $\alpha_{alkenone}$ and salinity, in contrast to culture results (Schouten et al., 2006; M'Boule et al., 2014; Sachs et al., 2016; Weiss et al., 2017). One explanation proposed by Schwab and Sachs (2011) for the lack of correlation between $\alpha_{alkenone}$ and salinity is the presence of different alkenone-producing species in the Chesapeake Bay Estuary. Indeed, coastal alkenone-producing haptophyte species are characterized by more enriched δ^2H_{C37} ratios and higher $\alpha_{alkenone}$ values (less fractionation) compared to marine alkenone-producing haptophytes (Chivall et al., 2014; M'Boule et al., 2014). Therefore, contributions from both groups of alkenone-producers can mute the correlation between $\alpha_{alkenone}$ and salinity. Suspended particulate matter (SPM) was also analyzed for δ^2H_{C37} ratios along a transect in the North Atlantic and shows that both δ^2H_{C37} ratios and α_{C37} values correlate with salinity, but only for SPM with an alkenone concentration >10 ng L^{-1} (Häggi et al., 2015). The correlation with higher alkenone concentrations suggests that alkenones have been produced predominantly *in situ* when concentrations are higher. No correlation is observed for concentrations <10 ng L^{-1} because the alkenones potentially represent a recalcitrant alkenone pool transported from elsewhere. Alkenones are known to be relatively recalcitrant and can therefore be transported laterally over rather long distances (Ohkouchi et al., 2002).

Here we test the relationship between hydrogen isotope ratios of alkenones and salinity by measuring hydrogen isotope ratios of alkenones preserved in surface sediments from four marine environments covering an annual mean sea surface salinity range from 7 to 39. Because these sediments are from areas covering a large salinity gradient, they also cover a range of temperature and light conditions, as well as differences in nutrient composition, evaporation and precipitation and species composition. This allows us to test if these variables affect the relationship between hydrogen isotopic composition of alkenones and salinity in the natural marine environment.

2. METHODS

Surface sediments (0–1 cm) were collected in triplicate using a multicorer aboard the RV Pelagia during six separate cruises: (1) to the Southeast North Atlantic (North Atlantic), (2) the Mediterranean Sea (in two legs) from Cyprus to Cadiz, Spain (Mediterranean), (3) the North Sea through the Skaggerak, Kattegat and into the Baltic Sea (Baltic), and the (4) the two campaigns in the Black Sea (Fig. 1). The surface sediments were freeze-dried and lipids were extracted via Accelerated Solvent Extraction (Dionex ASE 200) using dichloromethane:methanol (9:1, v/v) at 100 °C with a pressure of 7.6×10^6 Pa. Total lipid extracts were separated into apolar, ketone and polar fractions using a small aluminum oxide column following Weiss et al. (2017).

2.1. North Atlantic

Alkenones from North Atlantic surface sediments were quantified using an Agilent 6890 gas chromatograph coupled to a flame ionization detector (GC-FID) with helium as a carrier gas. Hydrogen isotope measurements were conducted using Thermo Finnigan DELTA V GC/TC/irMS. Both GCs were equipped with a CPSil5 column (Agilent, 25 m × 0.32 mm × 0.4 μm), using the same temperature program as M'Boule et al. (2014). Prior to running samples for isotope ratios each day, the H_3^+ factor was measured and ranged between 4.4 and 5.4 ppm V^{-1}, with a variation of less than 0.2 ppm V^{-1} from day to day. An external standard, Mix B (supplied by A. Schimmelmann, Indiana University), was run each day prior to running samples. Samples were only analyzed when the average difference from the offline values and standard deviation of the Mix B were less than 5‰. Squalane and a C_{30} n-alkane were co-injected with each hydrogen isotope run, and values had an average δ^2H ratio of -158.7 ± 5.8 (squalane) and -77.9 ± 8.0 (C_{30} n-alkane); standard deviations are relatively high for this sample set due to the comparatively high and variable background with co-eluting compounds in these samples at or close to the time squalane and C_{30} elute from the column. Ketone fractions from the same sampling station were combined prior to hydrogen isotope measurement when alkenone abundance was too low (based on GC-FID quantification). The reported isotope ratios and standard deviations are the average of duplicate measurements. Due to the lack of baseline

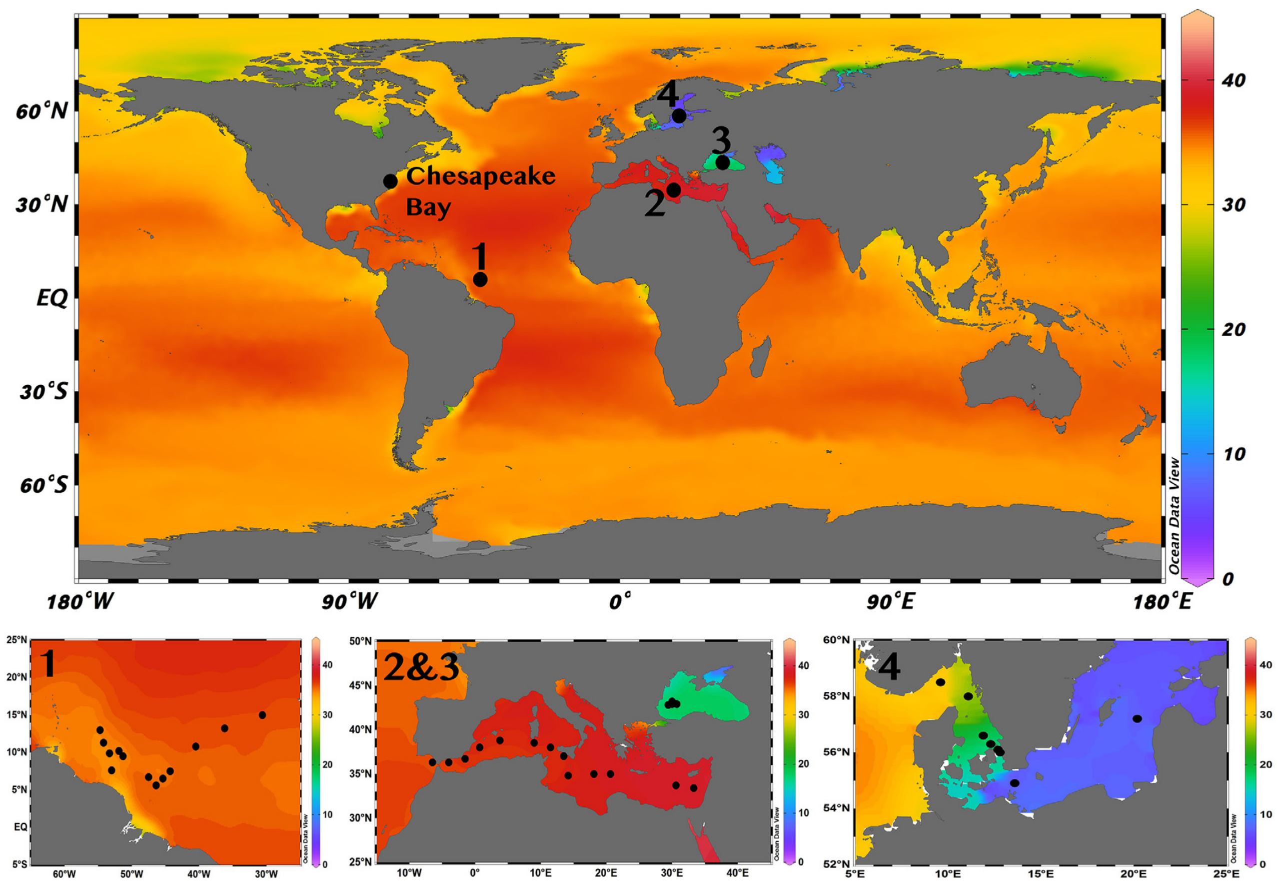

Fig. 1. Global map of annual mean salinity values from the World Ocean Atlas 2013 with 0.25° grid resolution with locations of transects. (1) North Atlantic transect (North Atlantic) into Amazon River outflow with annual mean salinity from 33 to 36.5. (2) Mediterranean Sea (Mediterranean) transect covering annual mean salinity of 36.5–39 (Mediterranean). (3) Black Sea with an annual mean salinity of 18. (4) North Sea into the Baltic Sea transect (Baltic) covering annual mean salinity from 30 (N. Sea) to 7 (Baltic). Previously published data for North Sea into the Baltic Sea (Kaiser et al., 2017) and Chesapeake Bay Estuary (Schwab and Sachs, 2011) also included. Specific sampling locations shown in lower panel.

separation with the CPSil5 GC column, we report only the isotope ratios of combined C_{37} alkenones for these samples (following van der Meer et al., 2013).

2.2. Mediterranean Sea, Baltic Sea and Black Sea

For alkenone quantification of the Mediterranean Sea, Baltic Sea and Black Sea sediments, ketone fractions were run on an Agilent 6890 GC-FID equipped with an RTX-200 column (Restek, 60 m × 0.32 mm × 0.5 μm), which allowed improved separation of alkenones with different chain lengths and degrees of unsaturation, similar to Longo et al. (2013), but with slightly different column dimensions (see Supplementary Fig. 1 for comparison of separated and integrated δ^2H ratios). The GC temperature program was as follows: 70 °C to 250 at 18 °C/min, 250–320 °C at 1.5 °C/min, then 320 °C for 25 °C/min at a flow rate of 1.5 mL/min.

For additional cleanup of the alkenones prior to δ^2H measurements, we separated the ketone fractions over a silver nitrate impregnated silica column using the following solvents: 100% dichloromethane, dichloromethane/ethyl acetate (1:1, v/v) and 100% ethyl acetate, with the alkenones ending up in the dichloromethane/ethyl acetate fraction. This clean-up step was especially necessary for the Mediterranean samples which contained high and variable backgrounds.

Alkenone quantification (Supplementary Table 1) was sufficient for determination of the $U^{K'}_{37}$ index (Fig. 2, Supplementary Table 2), but was often too low for duplicate δ^2H measurements. For this reason, ketone fractions from the same sampling station were combined when necessary prior to measurements of isotope ratios. Ketone fractions from Mediterranean Sea sediment extracts were run on GC-FID using both CPSil5 and RTX-200 columns to determine whether significant differences occur for calculation of the $U^{K'}_{37}$ index between columns (Supplementary Table 3).

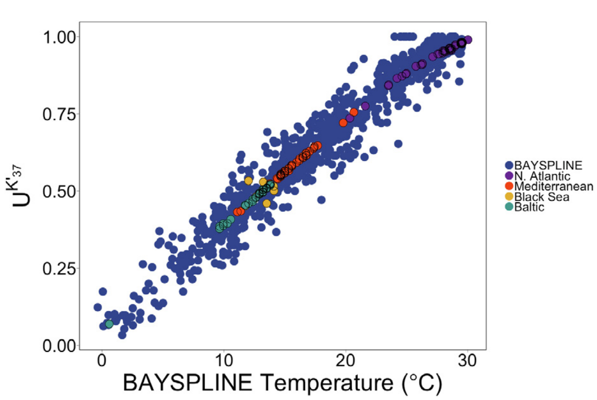

Fig. 2. $U^{K'}_{37}$ index calculated for our dataset calibrated to temperature using BAYSPLINE (Tierney and Tingley, 2018), and colored by transect. $U^{K'}_{37}$ values for our dataset are plotted with core-top values from the BAYSPLINE calibration. The fact that our values align well with the BAYSPLINE compilation confirms that our dataset strongly reflects surface water conditions. (For interpretation of the references to colour in this figure legend, the reader is referred to the web version of this article.)

Hydrogen isotope ratios of alkenones were measured on a Thermo Finnigan DELTA V GC/TC/irMS with an RTX-200 column using the same GC temperature program as described above for GC-FID. The H_3^+ factor varied from 4.2 to 5.2 ppm V^{-1} for the Mediterranean Sea, 2.9–3.0 ppm V^{-1} for the Black Sea, and 2.4–4.5 for the Baltic Sea. The larger ranges are due to cleaning and tuning of the ion source in between analyzing sample batches while day to day variation was <0.2 ppm V^{-1}. As with the North Atlantic samples, an external Mix B standard was run each day before measuring samples, and we only proceeded with running samples once the average difference from the offline values and standard deviation of the Mix B were less than 5‰. An in house alkenone mix was run periodically to further assess machine stability. Squalane and a C_{30} n-alkane were co-injected with each run; δ^2H values for the Mediterranean sample series had an average of -171.9 ± 3.9 (squalane) and -78.0 ± 4.6 (C_{30} n-alkane), the Baltic Sea sample series had an average of -166.2 ± 2.9 (squalane) and -71.3 ± 2.5 (C_{30} n-alkane), and the Black Sea sample series had an average of -165.8 ± 1.9 (squalane) and -69.2 ± 1.4 (C_{30} n-alkane). Isotope ratios for the individual alkenones are reported (Table 1, Supplementary Fig. 1), but we use the values of the integrated C_{37} alkenones for statistical comparisons with the North Atlantic samples and previously published Baltic Sea data (Kaiser et al., 2017). Reported isotope ratios and standard deviations are the average of duplicate analytical runs.

2.3. Sea surface water isotopes, salinity and temperature

Water samples were collected from surface waters at the same location that the sediment samples were taken, and salinity, temperature and δ^2H_{H2O} ratios were measured. δ^2H_{H2O} ratios were measured using TC/EA/irMS following methods of M'Boule et al. (2014). Water was not collected for isotopic analyses along the North Atlantic transect, therefore, we estimated δ^2H_{H2O} ratios using the Schmidt et al. (1999) Global Seawater Oxygen isotope database and the global meteoric waterline equation following Craig and Gordon (1965):

$$\delta^2H_{H2O} = 8 \times \delta^{18}O_{H2O} + 10 \quad (1)$$

Hydrogen isotope fractionation factor α_{C37} was calculated for all samples using the equation:

$$\alpha_{C37} = \frac{\delta^2H_{C37} + 1000}{\delta^2H_{H2O} + 1000} \quad (2)$$

Seasonal and annual mean sea surface temperatures and salinity were taken from the World Ocean Atlas (Antonov et al., 2010; Locarnini et al., 2010).

3. RESULTS

3.1. Sea water

δ^2H_{H2O} ratios, temperature, and salinity of surface waters were measured at each sampling station where sediment was collected, except for the North Atlantic transect

Table 1
Hydrogen isotope ratios of surface water and long-chain alkenones and surface water parameters for North Atlantic, Mediterranean, Black and Baltic Sea transects.

Location	Station	Sample	Latitude (°N)	Longitude (°E)	$\delta^2H_{C37:3}$ (‰ vs. VSMOW)	S.D.	$\delta^2H_{C37:2}$ (‰ vs. VSMOW)	S.D.	Combined δ^2H_{C37} (‰ vs. VSMOW)	S.D.	Measured salinity	Measured temperature	δ^2H_{H2O} (‰ vs. VSMOW)	S.D.	α_{C37}	S.E.	WOA annual mean salinity	S.E.
North Atlantic	1	1a	15.0	−30.6	–	–	–	–	−178	0	36.4	27.1	10	–	0.806	–	36.3	0.0
		1b			–	–	–	–	−186	1				–	0.814	–	36.3	0.0
	3	3a	13.2	−36.2	–	–	–	–	−180	0	36.4	27.3	10	–	0.812	–	36.3	0.1
	5	5a	10.8	−40.5	–	–	–	–	−179	0	36.0	28.0	10	–	0.813	–	35.9	0.1
		5b			–	–	–	–	−195	4				–	0.797	–	35.9	0.1
	7	7a	7.5	−44.3	–	–	–	–	−173	1	32.6	29.2	6	–	0.822	–	35.6	0.1
		7b			–	–	–	–	−159	2				–	0.836	–	35.6	0.1
	8	8a	6.5	−45.4	–	–	–	–	−164	0	31.9	29.2	6	–	0.832	–	35.0	0.4
		8b			–	–	–	–	−176	5				–	0.82	–	35.0	0.4
	9	9a	5.6	−46.4	–	–	–	–	−170	7	31.4	28.9	6	–	0.825	–	35.7	0.2
		9b			–	–	–	–	−178	2				–	0.817	–	35.7	0.2
	10	10a	6.7	−47.5	–	–	–	–	−182	7	31.3	29.4	6	–	0.814	–	35.4	0.1
		10b			–	–	–	–	−179	0				–	0.817	–	35.4	0.1
	13	13a	7.6	−53.0	–	–	–	–	−188	0	32.8	28.0	6	–	0.807	–	34.3	0.3
		13b			–	–	–	–	−182	1				–	0.813	–	34.3	0.3
		13c			–	–	–	–	−189	2				–	0.807	–	34.3	0.3
	14	14a	9.5	−51.3	–	–	–	–	−185	0	31.6	28.5	6	–	0.814	–	35.0	0.2
		14b			–	–	–	–	−181	2				–	0.81	–	35.0	0.2
	16	16a	10.2	−51.9	–	–	–	–	−183	2	33.9	29.2	6	–	0.812	–	35.1	0.1
	17	17a	9.9	−53.3	–	–	–	–	−181	1	31.6	29.0	6	–	0.814	–	34.9	0.3
		17b			–	–	–	–	−175	2				–	0.82	–	34.9	0.3
	20	20a	11.3	−54.2	–	–	–	–	−155	2	33.9	29.2	6	–	0.811	–	35.0	0.4
		20b			–	–	–	–	−184	1				–	0.84	–	35.0	0.4
	21	21a	11.3	−54.2	–	–	–	–	−157	2	33.8	28.9	6	–	0.838	–	35.0	0.4
Mediterranean	406-1	E_1a	33.3	33.4	−178	2	−180	2	−181	5	39.0	19.0	14	2	0.807	0.003	39.1	0.0
	406-2	E_2a	33.7	30.6	−156	9	−170	1	−173	3	39.0	18.0	12	4	0.817	0.003	39.0	0.0
	406-5	E_5a	35.0	20.6	−175	1	−176	3	−177	2	39.1	17.0	9	2	0.815	0.002	38.6	0.0
		E_5b			−146	14	−155	7	−157	10				2	0.835	0.004	38.6	0.0
	407-1	W_1a	34.8	14.2	−176	6	−186	3	−184	2	37.8	17.0	15	3	0.804	0.002	37.9	0.1
	407-2	W_2a	37.0	13.5	−184	8	−177	1	−183	6	38.2	15.2	11	2	0.808	0.003	37.3	0.0
		W_2b			−183	1	−177	6	−182	5				2	0.809	0.003	37.3	0.0
		W_2c			−180	3	−183	4	−182	4				2	0.809	0.003	37.3	0.0
	407-3	W_3a	38.0	11.5	−180	4	−179	1	−176	1	38.0	15.0	10	2	0.816	0.002	37.6	0.0
		W_3b			−186	3	−180	2	−183	3				2	0.809	0.002	37.6	0.0
	407-4	W_4a	38.5	9.0	−186	5	−170	7	−184	5	38.2	14.6	11	3	0.807	0.003	37.7	0.0
		W_4b			−166	5	−170	5	−167	4				3	0.824	0.003	37.7	0.0
	407-6	W_6a	38.8	3.8	−177	5	−177	3	−177	5	37.2	15.5	9	2	0.816	0.003	37.3	0.0
	407-7	W_7a	38.0	0.7	−194	1	−194	2	−193	1	37.3	15.5	11	2	0.799	0.002	37.5	0.0

		W_7b			−187	4	−179	21	−189	3				2	0.803	0.002	37.5	0.0
	407-8	W_8a	36.7	−1.5	−185	2	−172	3	−182	0	37.9	14.0	11	2	0.810	0.002	37.0	0.0
		W_8b			−184	6	−184	4	−183	5				2	0.808	0.003	37.0	0.0
		W_8c			−183	0	−186	1	−183	1				2	0.808	0.002	37.0	0.0
	407-9	W_9a	36.3	−4.0	−178	1	−179	2	−178	1	36.8	15.2	7	1	0.817	0.002	37.0	0.0
		W_9b			−170	6	−172	12	−172	6				1	0.823	0.003	37.0	0.0
		W_9c			−173	7	−167	20	−173	12				1	0.822	0.004	37.0	0.0
	407-10	W_10a	36.3	−6.5	−179	2	−179	9	−179	3	36.0	15.0	10	3	0.813	0.003	36.1	0.0
		W_10b			−179	4	−185	3	−183	0				3	0.809	0.002	36.1	0.0
		W_10c			−177	3	−171	12	−176	3				3	0.817	0.003	36.1	0.0
		W_10d			−173	0	−180	1	−177	1				3	0.815	0.002	36.1	0.0
Black	12	12a	42.9	30.0	−218	0	−221	1	−219	0	18.5	8.3	−18	2	0.796	0.002	18.2	0.2
		12b			−211	1	−215	2	−213	2				2	0.802	0.002	18.2	0.2
	2	2a	42.9	30.7	−215	1	−216	1	−215	1	18.5	8.3	−18	2	0.799	0.002	18.2	0.2
		2b			−217	0	−218	0	−217	0				2	0.797	0.002	18.2	0.2
		2c			−220	2	−221	2	−220	2				2	0.794	0.002	18.2	0.2
	4	4a	42.8	29.4	−218	3	−220	3	−219	3	18.5	9.4	−18	2	0.795	0.003	18.2	0.4
		4b			−214	0	−219	1	−217	1				2	0.798	0.002	18.2	0.4
Baltic	1	1a	58.5	9.6	−182	2	−177	1	−180	3	30.0	11.5	−9	1	0.828	0.002	27.9	0.1
		1b			−181	2	−181	4	−180	1				1	0.828	0.002	27.9	0.1
	2	2a	58.0	11.1	−190	0	−192	2	−190	1	26.0	11.5	−15	1	0.822	0.002	27.9	0.1
		2b			−189	1	−199	0	−194	1				1	0.819	0.001	27.9	0.1
		2c			−188	1	−184	4	−186	2				1	0.827	0.002	27.9	0.1
	3	3a	56.6	11.9	−215	1	−208	4	−212	1	16.1	11.5	−32	1	0.814	0.001	19.5	0.1
		3b			−206	7	−203	7	−204	7				1	0.822	0.003	19.5	0.1
		3c			−211	5	−218	2	−214	3				1	0.812	0.003	19.5	0.1
	4	4a	56.3	12.3	−213	5	−217	4	−215	4	17.5	10.7	−30	1	0.809	0.003	19.5	0.1
		4b			−209	0	−215	1	−213	1				1	0.812	0.002	19.5	0.1
		4c			−216	7	−220	7	−218	7				1	0.806	0.003	19.5	0.1
	5	5a	56.1	12.7	−214	8	−210	6	−217	9	18.5	11.2	−27	1	0.805	0.004	19.5	0.1
		5b			−225	0	−227	1	−226	1				1	0.796	0.001	19.5	0.1
		5c			−221	0	−221	1	−220	1				1	0.802	0.001	19.5	0.1
	6	6a	56.0	12.8	−222	11	−221	12	−222	11	12.2	12.0	−39	1	0.810	0.004	19.5	0.1
		6b			−224	8	−232	1	−225	8				1	0.807	0.004	19.5	0.1
		6c			−223	2	−227	1	−226	0				1	0.806	0.001	19.5	0.1
	7	7a	54.9	13.6	−222	8	−221	11	−223	8	8.3	11.9	−47	0	0.818	0.004	8.1	0.0
		7b			−225	1	−226	1	−226	0				0	0.813	0.001	8.1	0.0
	10	10a	57.2	20.2	−184	1	−177	3	−181	2	7.0	11.6	−51	1	0.864	0.002	6.6	0.0

where only temperature and salinity were measured. Temperature ranged from 27.1 to 29.4 °C for the North Atlantic, 14.0–19.0 °C for the Mediterranean, 8.3 °C for the Black Sea, and 10.6–11.9 °C for the Baltic; salinity ranged from 31.1 to 36.4 for the North Atlantic, 36–39 for the Mediterranean, 18.5 for the Black Sea and 7–30 for the Baltic; δ^2H_{H2O} ratios ranged from 6 to 10‰ for the North Atlantic, 7–14‰ for the Mediterranean, −18‰ for the Black Sea, and −51 to −9‰ for the Baltic Sea (Table 1). As mentioned in the introduction, a strong correlation between δ^2H_{H2O} and salinity is expected for surface ocean waters, as both are impacted in a similar fashion by the hydrological cycle (Craig and Gordon, 1965; Fröhlich et al., 1988). Indeed, for the combined Mediterranean, Black Sea, and Baltic Sea transects, where we measured both δ^2H_{H2O} and salinity at each sampling location, there is a strong significant relationship between measured salinity and δ^2H_{H2O} ($r = 0.99$, $p < 0.001$; Fig. 3a). When using the Schmidt et al. (1999) database to estimate δD_{H2O} for the North Atlantic transect (where only salinity was measured at each sampling location), the correlation still remains highly significant ($r = 0.98$, $p < 0.001$).

3.2. $U^{K'}_{37}$ values

$U^{K'}_{37}$ index values were determined on a standard CPSil5 25 m as well as on a 60 m RTX-200 GC column, which we also used for compound specific hydrogen isotope analysis. To determine if the $U^{K'}_{37}$ index values measured on the two GC columns were different, we ran all Mediterranean samples on both columns (Supplementary Table 3). Using the student t-test, we determined that the differences between the $U^{K'}_{37}$ index calculated based on analyses from both columns are not statistically different. Therefore, we can compare the $U^{K'}_{37}$ index from the North Atlantic (measured on the CPSil5 column) with those from the other transects (measured on the RTX-200 column). The $U^{K'}_{37}$ index ranges from 0.74 to 0.99 for the North Atlantic, from 0.50 to 0.76 for the Mediterranean from 0.45 to 0.53 for the Black Sea, and 0.07–0.52 for the Baltic Sea (Supplementary Table 2). $U^{K'}_{37}$ index was converted to temperatures using the BAYSPLINE calibration (Tierney and Tingley, 2018). Temperatures range from 20.3 °C to 30.0 °C for the North Atlantic, 11.1–20.7 °C for the Mediterranean, 11.8–14.1 °C for the Black Sea and 0.6–13.8 °C for the Baltic Sea (Fig. 2).

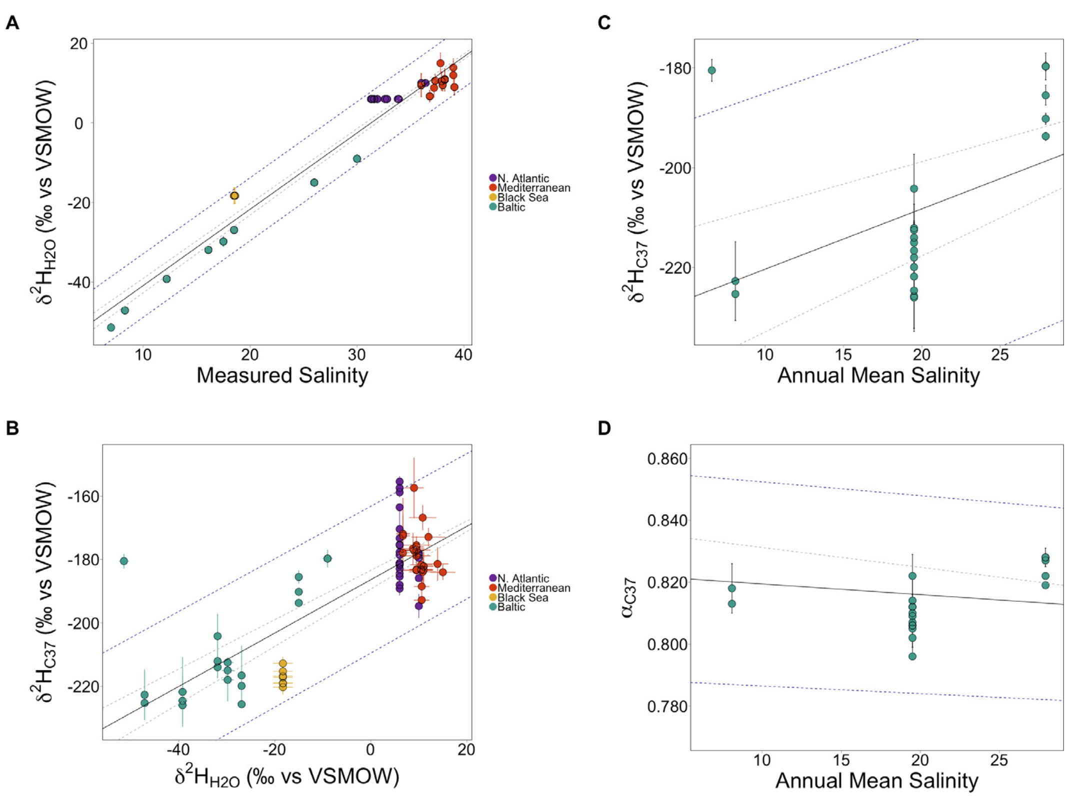

Fig. 3. Surface water salinity measured during sampling plotted against hydrogen isotope ratios of surface water also collected during sampling for all transects are shown in (A), with estimated water isotope values for the North Atlantic Transect from Schmidt et al. (1999). (B) Shows water isotope ratios of surface water plotted against hydrogen isotope ratios of alkenones extracted from surface sediments for all transects. Results for the correlation between annual mean salinity and δ^2H_{C37} for the Baltic Sea transect are shown in (C) and α_{C37} is plotted against annual mean salinity for the Baltic Sea transect in (D). Annual mean salinity values were taken from the World Ocean Atlas (Antonov et al., 2010; Locarnini et al., 2010). Y-axis errors are the standard deviations of duplicate analyses and X-axis errors are the standard errors of the statistical mean for the 0.25° gridded WOA annual mean salinity dataset.

3.3. Correlations of hydrogen isotope ratios and fractionation with salinity

Correlations between δ^2H_{C37} ratios and salinity for individual transects are all poor with p values that are not significant (Table 2). The relationships between α_{C37} and salinity are likewise not statistically significant for the individual transects. The Baltic Sea is an exception, probably as a result of the larger salinity gradient covered by this transect. There is a significant positive correlation between δ^2H_{C37} ratios with annual mean salinity ($r = 0.83$, $p < 0.001$). When previously published marine surface sediment data from the Chesapeake Bay Estuary, USA (transformed to the weighted mean C_{37} value by using reported $U^{K'}_{37}$ and individual δ^2H_{C37} ratios from Schwab and Sachs, 2011) and the Baltic Sea (Kaiser et al., 2017) are included ($n = 18$), there remains a significant correlation with annual mean salinity ($r = 0.75$, $p < 0.001$). The correlation between δ^2H_{C37} – annual mean salinity is characterized by the linear regression equation:

$$\delta^2H_{C37} = 1.3 \times S - 227(R^2 = 0.55,\ p < 0.001,\ n = 95;\ \text{Fig. 4(a)} \quad (3)$$

For the combined dataset, there is a weak negative correlation between α_{C37} and annual mean salinity ($r = -0.27$, $p < 0.05$; Fig. 4(b)).

4. DISCUSSION

4.1. $U^{K'}_{37}$ temperatures

The $U^{K'}_{37}$ index is a well-known and well-studied proxy for sea surface temperature (SST) (Brassell et al., 1986; Müller et al., 1998; Tierney and Tingley, 2018). Although $U^{K'}_{37}$ is shown to vary with depth of alkenone production, alkenones preserved in sediments are strongly reflecting surface mixed layer conditions (Prahl et al., 2005). To calibrate $U^{K'}_{37}$ values to SSTs, we used the BAYSPLINE regression model, which is more accurate than previous calibrations for temperatures above 24 °C (Tierney and Tingley, 2018).

Table 2
Pearson's correlation coefficient (r) and p-values for strongest correlations between δ^2H_{C37} and α_{C37} with annual mean and seasonal salinity for individual transects. Correlations between δ^2H_{C37} and α_{C37} with annual mean and seasonal salinity, temperature, and nutrients for combined dataset, including previously published data from Schwab and Sachs (2011) and Kaiser et al. (2017). Table 2 also shows r and p-values for $U^{K'}_{37}$ values correlated to annual mean and seasonal temperatures.

	Parameters	R	p value
North Altantic	δ^2H_{C37} vs. spring salinity	−0.17	>0.05
	α_{C37} vs. spring salinity	−0.20	>0.05
Mediterranean	δ^2H_{C37} vs. summer salinity	0.27	>0.05
	α_{C37} vs. spring salinity	0.15	>0.05
	α_{C37} vs. summer salinity	0.15	>0.05
Black Sea	δ^2H_{C37} vs. fall salinity	0.35	>0.05
	δ^2H_{C37} vs. winter salinity	0.35	>0.05
	α_{C37} vs. fall salinity	0.44	>0.05
	α_{C37} vs. winter salinity	0.44	>0.05
Baltic Sea	δ^2H_{C37} vs. spring salinity	0.52	<0.05
	α_{C37} vs. fall salinity	−0.63	<0.01
This study and previously published results from Schwab and Sachs (2011) & Kaiser et al. (2017)	δ^2H_{C37} vs. annual mean salinity	0.75	<0.001
	δ^2H_{C37} vs. spring salinity	0.75	<0.001
	δ^2H_{C37} vs. summer salinity	0.75	<0.001
	δ^2H_{C37} vs. fall salinity	0.71	<0.001
	δ^2H_{C37} vs. winter salinity	0.70	<0.001
	α_{C37} vs. annual mean salinity	−0.27	<0.05
	α_{C37} vs. spring salinity	−0.28	<0.05
	α_{C37} vs. summer salinity	−0.27	<0.05
	α_{C37} vs. fall salinity	−0.31	<0.05
	α_{C37} vs. winter salinity	−0.31	<0.05
Temperature	δ^2H_{C37} vs. fall temperature	0.75	<0.001
	δ^2H_{C37} vs. winter temperature	0.74	<0.001
	α_{C37} vs. fall temperature	0.32	<0.01
	α_{C37} vs. winter temperature	0.34	<0.01
Nutrients	δ^2H_{C37} vs. annual mean N	−0.5	<0.001
	δ^2H_{C37} vs. annual mean P	−0.8	<0.001
	α_{C37} vs. annual mean N	−0.1	>0.05
	α_{C37} vs. annual mean P	−0.1	>0.05
	Annual mean S vs. annual mean P	−0.8	<0.001
$U^{K'}_{37}$	$U^{K'}_{37}$ vs. annual mean temperature	0.89	$p < 0.001$
	$U^{K'}_{37}$ vs. spring temperature	0.92	$p < 0.001$

The $U^{K'}_{37}$-SST relationship for this dataset aligns nicely with the compilation of global core-top $U^{K'}_{37}$ SST values (Tierney and Tingley, 2018; Fig. 2), which leads to the conclusion that alkenones along these transects are also recording surface water values. In general, nannoplankton blooms, which include haptophytes, occur during the spring, following a bloom of diatoms (Lochte et al., 1993). In the Eastern Mediterranean, coccolithophore production reaches a maximum between late winter and early spring (Ziveri et al., 2000) and the largest haptophyte blooms in the Western Mediterranean occur in fall (Knappertsbusch, 1993; Cacho et al., 1999). To determine if the sedimentary alkenones from the compiled dataset are affected by differences in seasonality due to the seasonal production of alkenones, we tested how well the $U^{K'}_{37}$ index correlates with annual mean and seasonal mean surface water temperatures from the World Ocean Atlas. $U^{K'}_{37}$ values correlate positively to both spring and annual mean temperatures ($r = 0.89$ for annual and $r = 0.92$ for spring), allowing us to conclude that alkenones preserved along these transects are reflecting surface water conditions and δ^2H_{C37} ratios do not contain a strong seasonality signal.

4.2. Hydrogen isotope ratios of alkenones

To test how accurately δ^2H_{C37} ratios are tracking surface water isotope ratios, we first compared the δ^2H_{C37} ratios of the sediments with the δ^2H_{H2O} ratios measured in surface water at the sampling locations. Sedimentary alkenones represent possible lateral transport (Ohkouchi et al., 2002) and accumulation over several decades to centuries, while the water signal covers several weeks to months. Nonetheless, there is a positive linear correlation ($r = 0.80$, $p < 0.001$) between surface water isotope ratios and δ^2H_{C37}, represented by the linear regression equation:

$$\delta^2H_{C37} = 0.84 \times \delta^2H_{H2O} - -186\ (R^2 = 0.64,\ p < 0.001,\ n = 75;\ \text{Fig. 3(b)} \tag{4}$$

This confirms that our δ^2H_{C37} ratios are plausibly recording surface water conditions. Since the δ^2H_{C37} ratios of alkenones seem to be recording the δ^2H_{H2O} ratios of surface water, which itself is strongly correlated to salinity, a strong correlation between δ^2H_{C37} ratios and salinity is expected. Rather than using measured salinity from each sampling station, we used the seasonal mean and annual mean salinities from the World Ocean Atlas to better align with an integrated sedimentary signal (Antonov et al., 2010; Locarnini et al., 2010). Because each transect covers a relatively small range of salinities, we focus on the combined transect. Our $U^{K'}_{37}$ values suggest that there is not a strong seasonal signal recorded by the alkenones for the combined dataset, and we observed the same for δ^2H_{C37} ratios (Table 2). The Baltic Sea transect covers a relatively large salinity range from approximately 7–30, and the δ^2H_{C37} ratios from the Baltic Sea transect correlate best with spring salinity ($r = 0.52$, $p < 0.05$; Fig. 3c). However, at lower salinities this overall positive correlation deviates from what is observed in culture studies (Schouten et al., 2006; M'Boule et al., 2014; Sachs et al., 2016). δ^2H_{C37} ratios are more enriched at lowest salinities, hinting that δ^2H_{C37} ratios might be influenced by some other variable. As mentioned above, we combined new data presented here with previously published data to extend the salinity gradient from 7 to 39. For the combined dataset, there is a significant, positive linear correlation between δ^2H_{C37} ratios with annual mean salinity (see Eq. (3), Table 2, Fig. 4).

In cultures, a strong correlation between hydrogen isotope fractionation factor α_{C37} values and salinity is reported (Schouten et al., 2006; Chivall et al., 2014; M'Boule et al.,

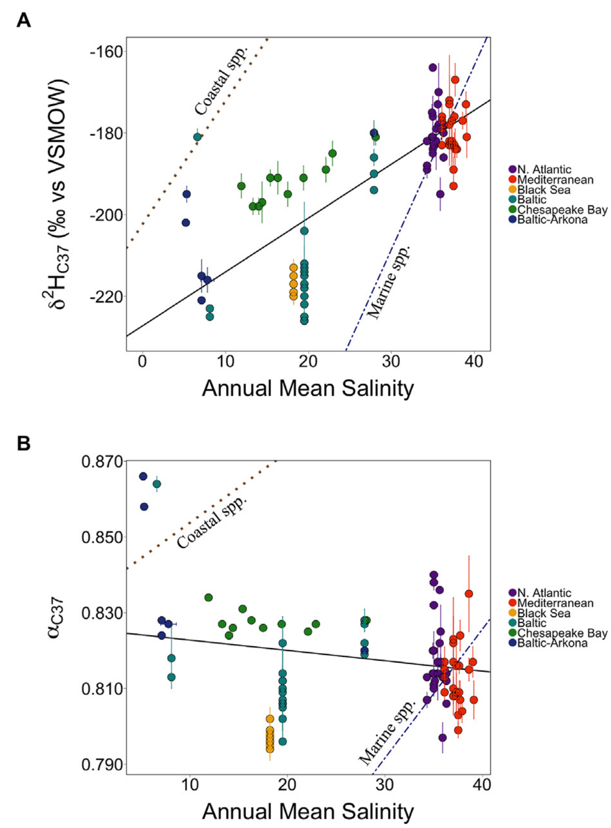

Fig. 4. Annual mean salinity plotted against (A) δ^2H_{C37} and (B) α_{C37} for all surface sediments (this study combined with previously published data from Schwab and Sachs, 2011; Kaiser et al., 2017) with linear regression equations from culture experiments with marine haptophyte alkenone-producers denoted by the dashed line (compiled in Weiss et al., 2017; includes data from Schouten et al., 2006, M'Boule et al., 2014, Sachs et al., 2016) and coastal haptophyte alkenone-producers designated by the dotted line (Chivall et al., 2014; M'Boule et al., 2014). Y-axis errors are the standard deviations of duplicate analyses and X-axis errors are the standard errors of the statistical mean for the 0.25° gridded WOA annual mean salinity dataset. North Atlantic and Mediterranean δ^2H_{C37} ratios fit with marine haptophyte culture data, and the lower salinity Baltic Sea and Chesapeake Bay Estuary δ^2H_{C37} ratios fit with coastal haptophyte culture values. δ^2H_{C37} and annual mean salinity for the World Ocean Atlas are strongly positively correlated ($r = 0.75$, $p < 0.001$). The linear regression equation that best fits the combined surface sediment data is: $\delta^2H_{C37} = 1.3\ S - 227$ ($R^2 = 0.55$, $p < 0.001$, $n = 95$). There is no significant correlation between salinity and α_{C37}.

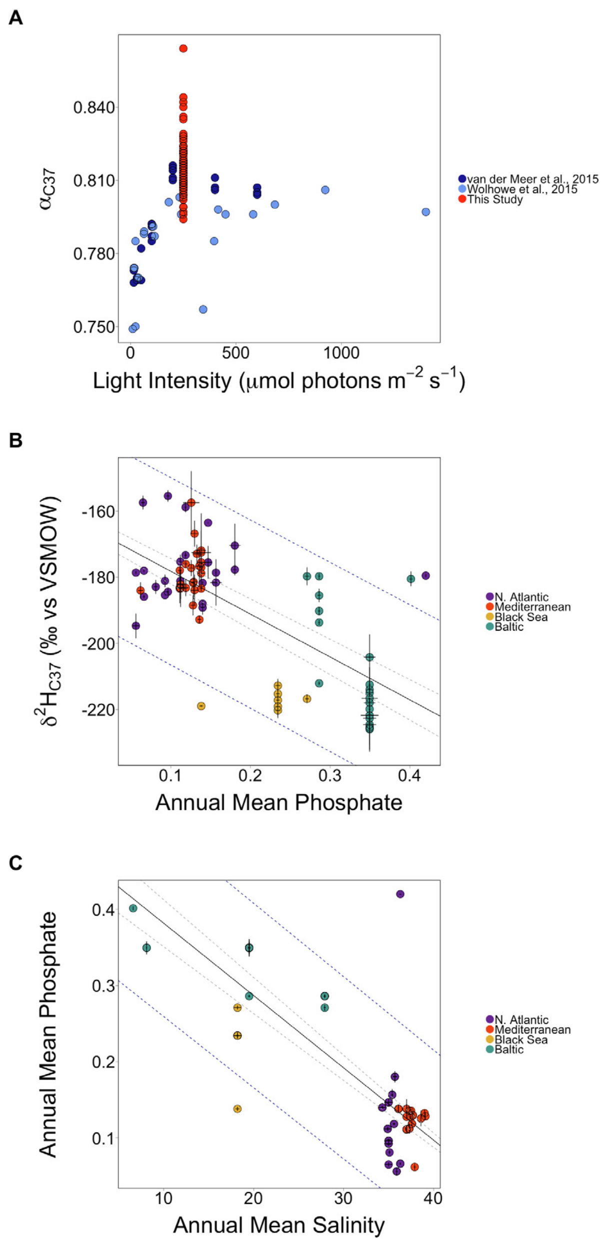

Fig. 5. Light intensity plotted against α_{C37} from cultures (van der Meer et al., 2015), suspended particulate matter (Wolhowe et al., 2015) and surface sediments (A). Annual mean phosphate is plotted against δ^2H_{C37} (B) and annual mean salinity (C). Annual mean phosphate and salinity values were taken from the World Ocean Atlas (Antonov et al., 2010, Locarnini et al., 2010; Garcia et al., 2010).

2014; Sachs et al., 2016; Weiss et al., 2017). Calculating α_{C37} values from sediment data is difficult as we do not have the δ^2H_{H2O} ratios over multiple years to decades. As a substitute, we used the δ^2H_{H2O} ratios of surface waters taken at the surface sediment sampling locations to roughly estimate α_{C37}. Surprisingly, we do not find a significant correlation between α_{C37} and annual mean or seasonal salinity (Table 2, Fig. 4b); seasonal correlations can be found in Table 2). A lack of correlation between α_{C37} and salinity has also been observed for alkenones in surface sediments of hypersaline lakes (Nelson and Sachs, 2014), and in the Chesapeake Bay Estuary (Schwab and Sachs, 2011) as well as in suspended particulate organic matter (SPOM) from a combined Atlantic and Pacific Ocean survey (Gould et al., 2019). The latter dataset includes alkenones produced by the two main open ocean haptophytes, *G. oceanica* and *E. huxleyi,* which are both shown to fractionate differently (Schouten et al., 2006). For the surface sediment datasets, the lack of correlation between α_{C37} and salinity is attributed to mixing of alkenones produced by haptophyte species from both marine and marginal marine environments. We explore the potential species effect on our dataset in Section 4.4.

4.3. Environmental factors impacting δ^2H of alkenones

Based on the $U^{K'}_{37}$ index, we infer that our dataset is reflecting surface water conditions. Indeed, we see a significant correlation between δ^2H_{C37} ratios and sea surface salinity, but no such correlation is observed between α_{C37} and salinity, a thought-provoking observation warranting further investigation. The North Atlantic surface sediments appear to have a much larger range in both δ^2H_{C37} ratios and α_{C37} values than expected based on the small range of annual mean salinity (34.8–36.5). In fact, the measured surface salinity is much larger (31–36.5) than annual mean salinity and captures the effect of the Amazon river outflow at the time of sampling. Freshwater from the Amazon river not only lowers surface salinities, but also likely transports haptophytes and the alkenones they produce from elsewhere. This may explain the >20‰ variation in δ^2H_{C37} ratios observed for the North Atlantic transect. A similar range in δ^2H_{C37} ratios was identified in suspended particulate matter along a nearby transect (Häggi et al., 2015). The large range in δ^2H_{C37} ratios and α_{C37} values might be a regional artefact and the result of lateral transport. Furthermore, as already noted, Baltic Sea sediments from lower salinities have more enriched δ^2H_{C37} ratios and deviate from the δ^2H_{C37} – salinity trend. As a consequence, factors other than salinity are conceivably affecting δ^2H_{C37} ratios and α_{C37} values and obscuring correlations. Therefore, we compared δ^2H_{C37} ratios and α_{C37} values with other environmental factors, like mean annual and seasonal temperatures and nutrients derived from the World Ocean Atlas (Antonov et al., 2010; Garcia et al., 2010; Locarnini et al., 2010) to determine the impacts of other environmental parameters on δ^2H_{C37} ratios and α_{C37} values.

In the natural environment, higher nutrient concentrations provide the potential for higher growth rates. To assess whether growth rate has an influence on our dataset, we tested the correlation between our δ^2H_{C37} ratios and α_{C37} values with annual mean nitrate (N) and phosphate (P) from the World Ocean Atlas (Antonov et al., 2010; Garcia et al., 2010). For our dataset, there is no correlation between α_{C37} values and either annual mean N or P, but there is a negative correlation between δ^2H_{C37} ratios and both annual mean N and P (Table 2). Higher nutrient values correspond to more depleted isotope ratios (Fig. 5), prompting further investigation about how growth rate effects might influence our dataset. Similar effects have been noted in chemostats of *E. huxleyi* via a correlation between higher nutrient composition and more depleted isotope ratios (Sachs and Kawka, 2015). To better understand the correlation between δ^2H_{C37} ratios and annual mean P, we examined the relationship between annual mean P and annual mean salinity. There is a strong negative correlation between annual mean salinity and annual mean P ($r = -0.84$, $p < 0.001$; Fig. 5), implying that the relationship between δ^2H_{C37} ratios and annual mean P is probably controlled by salinity. The correlation between annual mean salinity and annual mean P is anti-correlated to the δ^2H_{C37}-annual mean salinity correlation. Because of this, we propose that growth rate probably does not strongly influence the δ^2H_{C37} ratios for our dataset, and we suggest that this cannot explain the apparent lack of correlation between α_{C37} values and salinity.

Interestingly, there is a positive linear correlation with δ^2H_{C37} ratios and temperature, with more enriched values corresponding to higher temperatures (Table 2). The best correlations are with fall and winter temperature (fall: $r = 0.75$, $p < 0.0001$, winter: $r = 0.74$, $p < 0.0001$; Table 2). A moderate correlation is observed between α_{C37} values and temperature (Table 2). In culture, the effect of temperature is not well constrained. Some results suggest no effect of temperature on either δ^2H_{C37} ratios or α_{C37} values (Schouten et al., 2006). For other batch cultures, a negative correlation between temperature and both δ^2H_{C37} ratios and α_{C37} values is reported, meaning more enriched isotope ratios and less fractionation correspond to lower temperatures (Wolhowe et al., 2009). Because the culture results on the temperature effect are contradictory to one another and to what is observed in the field, it is difficult to confidently conclude that the temperature effect observed for our sample set is a true temperature effect. Furthermore, temperature and salinity are correlated with each other ($r = 0.75$, $p < 0.001$). The warmer regions have higher salinities and vice versa. Differences between evaporation and precipitation for the separate environments, for example between the evaporative Mediterranean Sea and the other transects, could be the cause of the strong correlation between δ^2H_{C37} ratios and temperature. Thus, the observed temperature relationship could possibly be an indirect correlation and not actually a temperature effect.

Light intensity has been shown to influence both δ^2H_{C37} ratios and α_{C37} values in culture and in the water column (van der Meer et al., 2015; Wolhowe et al., 2015). Wolhowe et al. (2015) report δ^2H_{C37} ratios and α_{C37} values from suspended particulate matter from the Gulf of California and Eastern Tropical North Pacific, and results show a depth effect on α_{C37} values, with lower depths corresponding to higher fractionation (lower α_{C37}). This depth effect is actually in all likelihood the effect of light intensity, since light intensities are lower at deeper depths. The trend between α_{C37} and depth in suspended particulate matter reported by Wolhowe et al. (2015) agrees with culture data assessing the effect of light intensity on α_{C37} values (van der Meer et al., 2015). α_{C37} values from our samples fall in the higher light range, above 200 μmols photons m^{-2} s^{-1}, where there is a negligible effect of light intensity (Fig. 5). We cannot completely rule out the effects of light and water depth on our sample set, but because α_{C37} values for our dataset align with α_{C37} values from higher light intensities (>200 μmol photons m^{-2} s^{-1}), we assume that the light and depth effects are minimal. Recent results from SPM in the North Pacific also suggest that light availability and nutrient limitation have a smaller effect on both δ^2H_{C37} ratios and α_{C37} values than has been shown in culture (Wolfshorndl et al., 2019), aligning with our conclusions that light and growth rate effects are negligible for the data presented here.

4.4. Species effect on δ^2H of alkenones

As mentioned above, it has been suggested that contributions from different alkenone-producing species caused the lack of correlation between α_{C37} and salinity in the Chesapeake Bay Estuary (Schwab and Sachs, 2011). Data from hypersaline lakes also show diminished sensitivity due to differences between lacustrine and marine alkenone producers (Nelson and Sachs, 214). Our findings are quite similar to these two datasets, i.e. a strong correlation of δ^2H_{C37} with salinity, but not of α_{C37} with salinity. The combination of data presented in this study and previous published results (Fig. 4) show that at higher salinities both δ^2H_{C37} ratios and α_{C37} values are similar to those found in *E. huxleyi* and *G. oceanica* culture experiments (Schouten et al., 2006; M'Boule et al., 2014; Sachs et al., 2016; Weiss et al., 2017). At the lowest salinities, δ^2H_{C37} ratios and α_{C37} values fit with culture experiments of *I. galbana* and *R. lamellosa* (Chivall et al., 2014; M'Boule et al., 2014), implying that differences between alkenone-producing haptophyte species could be important for our surface sediment dataset.

The Mediterranean and North Atlantic are characterized by high salinity (∼34–39) and the presence of *E. huxleyi* and *G. oceanica* (McIntyre and Bé, 1967; Knappertsbusch, 1993; Lomas and Bates, 2004), explaining why Mediterranean and North Atlantic δ^2H_{C37} ratios are in good agreement with *E. huxleyi* and *G. oceanica* culture data. For the modern day Black Sea, *E. huxleyi* is the only reported alkenone-producer (Moncheva et al., 2001), but both *E. huxleyi* and *G. oceanica* are absent from the present-day Baltic Sea (Tyrrell et al., 2008). Haptophytes have been reported to live in the Baltic Sea (Vepsäläinen et al., 2005). Previously reported alkenone patterns resemble those produced by *Ruttnera* and *Isochrysis* species (Conte et al., 1994; Schulz et al., 2000), and 18S rRNA analyses confirm the presence of both marine and coastal haptophyte groups in the Baltic Sea (Kaiser et al., 2019). Additionally, Baltic Sea alkenone distributions have a reported absence of C_{38} methyl alkenones, which are generally present in *E. huxleyi* and *G. oceanica* (Schulz et al., 2000). We also observe the absence of C_{38} methyl alkenones in some of our Gotland Basin sediments, suggesting a source other than *E. huxleyi* or *G. oceanica*. Indeed, the observed environmental salinity range for *E. huxleyi* is 11–41 (Brand, 1994; Schulz et al., 2000), and *G. oceanica* does not reproduce in salinities below 15 (Brand, 1984), so it is expected that *E. huxleyi* and *G. oceanica* will not live in the Baltic Sea. Moreover, the $C_{36:2}$ alkenone was

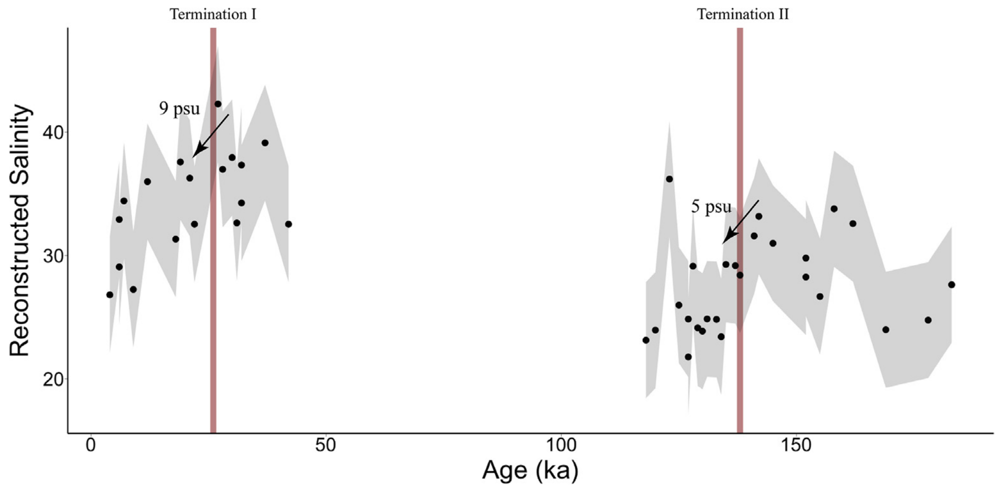

Fig. 6. Reconstructed salinities for the Agulhas Leakage (δ^2H_{C37} ratios published in Kasper et al., 2014) using the linear regression equation from the combined surface sediment dataset presented here. The surface sediment calibration results in a salinity shift of 9 psu across Termination I and 5 psu across Termination II.

detected in surface sediments from the Arkona basin in the Baltic Sea, as well as in Black Sea sediments. While the origin of the $C_{36:2}$ alkenone is not known, its presence always coincides with lower salinities, and is hypothesized to be from either *I. galbana* or a low salinity strain of *E. huxleyi* (Xu et al., 2001; Coolen and Gibson, 2009; Warden et al., 2016). Based on the presence of the $C_{36:2}$ alkenone and the absence of C_{38} methyl alkenones, we can conclude that different haptophyte species are contributing to the sedimentary alkenones in the Baltic Sea.

4.5. Implications

Our results show that α_{C37} values in marine surface sediments are not sensitive to salinity, opposite to observations from culture studies (Schouten et al., 2006; M'Boule et al., 2014; Sachs et al., 2016; Weiss et al., 2017) and some paleo settings (e.g. van der Meer et al., 2007). It appears that mixing of alkenones produced by different species is responsible for the lack of correlation between α_{C37} and salinity across our dataset. Alternatively, δ^2H_{C37} ratios from marine surface sediments compliment what has been observed in culture studies, and correlate significantly with sea surface salinity. Indeed, δ^2H_{C37} ratios have been used to track salinity changes for a number of paleo records (Pahnke et al., 2007; Leduc et al., 2013; Kasper et al., 2014; Kasper et al., 2015; Petrick et al., 2015; Simon et al., 2015). For these records, salinity is most commonly reconstructed using the slope of the δ^2H_{C37}-salinity relationship from Schouten et al. (2006) of 4.8 for *E. huxleyi* and 4.2 for *G. oceanica*, which are both much larger than the slope of 1.3 obtained for this dataset. To test the applicability of our surface sediment calibration for paleo settings, we have applied our calibration of δ^2H_{C37}-salinity to the δ^2H_{C37} record generated from a sediment core in the Agulhas leakage area (Kasper et al., 2014). As the amount of ice in ice sheets and glaciers around the globe varies (characterized by isotopically depleted values), the isotopic composition of the ocean (typically isotopically enriched) changes as a result (Chappell and Shackleton, 1986). Thus, in order to use δ^2H_{C37} ratios to calculate salinity values, the δ^2H_{C37} ratios must be corrected for global ice volume at the particular time period of interest. Kasper et al. (2014) corrected their δ^2H_{C37} ratios for global ice volume and calculated salinity changes using the slope of 4.8 from Schouten et al. (2006) to get a salinity change of 1.9 for Termination I and 1.7 for Termination II, which fits with salinity reconstructed from $\delta^{18}O_{foram}$ and Mg/Ca ratios measured on the same core. If we apply the slope of 1.3 from our surface sediment calibration, we obtain a salinity change of 9 across Termination I and 5 across Termination II (Fig. 6), much higher than reported values and $\delta^{18}O_{foram}$ and Mg/Ca reconstructions (Kasper et al., 2014). Not only does the surface sediment calibration result in large changes in salinity, but the propagated error for the calibration is 4.7, making it difficult to reconstruct the small changes in salinity expected for open ocean settings. This shows that our surface sediment calibration is substantially over-estimating changes in salinity. The surface sediment calibration presented here likely captures the effect of different haptophyte species, and therefore over-estimates paleo salinity shifts in open ocean settings where only marine haptophytes are presumed to contribute to the sedimentary alkenone record.

5. CONCLUSIONS

Based on the compilation of surface sediments from a range of environmental settings, we have shown that δ^2H_{C37} ratios have a strong positive linear correlation with annual mean sea surface salinity. However, α_{C37} values do not correlate with sea surface salinity, in contrast to previous findings from culture experiments. Other environmental factors, like temperature and nutrients, correlate with δ^2H_{C37} ratios, but also with salinity, implying an indirect relationship between these parameters and δ^2H_{C37} ratios, and possibly no effect on δ^2H_{C37} ratios. The most plausible explanation for the lack of correlation between α_{C37} and sea surface salinity is the difference in alkenone-producing haptophytes present in different locations. The δ^2H_{C37} ratios corresponding to lower salinities align nicely with culture data from coastal haptophyte species which are also reported to live in the low salinity environments along the different transects. The δ^2H_{C37} ratios corresponding to higher salinities fit nicely with the reported values for marine alkenone-producing species. Our results suggest that δ^2H_{C37} ratios might be a suitable proxy for sea surface salinity, especially in marginal marine environments where large ranges of salinity and mixing of alkenones from different alkenone-producing species is common. However, when applying δ^2H_{C37} ratios to estimate salinity for down-core records from open marine sites where smaller shifts in salinity and a stable alkenone-producing population are anticipated, the slope from our calibration provides salinity changes that are much larger than expected. While δ^2H_{C37} ratios can provide valuable information about past shifts in salinity, we emphasize that it can presently only be used to obtain qualitative estimates of salinity, rather than quantitative.

ACKNOWLEDGEMENTS

The captain and crew of the RV Pelagia are thanked for all of their help collecting samples. We would also like to thank the chief scientists of the Atlantic, Black Sea and Mediterranean transects, Nicole J. Bale, Laura Villanueva, and Gert Jan Reichart, respectively, for leading the sampling campaigns. We would like to thank Dr. Nemiah Ladd, two anonymous reviewers for their input which greatly improved this manuscript, as well as Associate Editor Dr. Jessica Tierney. This study received funding from the Netherlands Earth System Science Center (NESSC) though a Gravitation grant (024.002.001) from the Dutch Ministry for Education, Culture and Science. All acquired data will be stored in the Pangaea database.

APPENDIX A. SUPPLEMENTARY MATERIAL

Supplementary data to this article can be found online at https://doi.org/10.1016/j.gca.2019.01.038.

REFERENCES

Antonov J. I., Seidov D., Boyer T. P., Locarnini R. A., Mishonov A. V. and Garcia H. E. (2010) World Ocean Atlas 2009, Volume 2: Salinity. In *NOAA Atlas NESDIS 69* (ed. S. Levitus). S. Government Printing Office, Washington, D.C., p. 184.

Brand L. E. (1984) The salinity tolerance of forty-six marine phytoplankton isolates. *Estuar. Coast. Shelf S.* **18**, 543–556.

Brand L. E. (1994) Physiological ecology of marine coccolithophorids. In *Coccolithophores* (eds. A. Winter and W. G. Siesser). Cambridge Univ. Press, Cambridge, pp. 39–50.

Brassell S. C., Eglinton G., Marlowe I. T., Pflaumann U. and Sarnthein M. (1986) Molecular stratigraphy: a new tool for climatic assessment. *Nature* **320**, 129–133.

Cacho I., Pelejero C., Grimalt J. O., Calafat A. and Canals M. (1999) C37 alkenone measurements of sea surface temperature in the Gulf of Lions (NW Mediterranean). *Org. Geochem.* **30**, 557–566.

Chappell J. and Shackleton N. (1986) Oxygen isotopes and sea level. *Nature* **324**, 137.

Chivall D., M'Boule D., Sinke-Schoen D., Sinninghe Damsté J. S., Schouten S. and van der Meer M. T. J. (2014) The effects of growth phase and salinity on the hydrogen isotopic composition of alkenones produced by coastal haptophyte algae. *Geochim. Cosmochim. Ac.* **140**, 381–390.

Conte M. H., Volkman J. K. and Eglinton G. (1994) Lipid biomarkers of the Haptophyta. In *The Haptophyte Algae* (eds. J. C. Green and B. S. C. Leadbeater). Clarendon Press, Oxford, pp. 351–377.

Coolen M. J. and Gibson J. A. (2009) Ancient DNA in lake sediment records. *PAGES News* **17**, 104–106.

Craig H. and Gordon L. I. (1965) Deuterium and oxygen 18 variations in the ocean and the marine atmosphere. In *Stable Isotopes in Oceanographic Studies and Paleotemperatures* (ed. E. Tongiorgi). Consiglio nazionale delle ricerche, Spoleto, pp. 9–130.

De Leeuw J. W., van der Meer F. W., Rijpstra W. I. C. and Schenck P. A. (1980) On the occurrence and structural identification of long chain unsaturated ketones and hydrocarbons in sediments. In *Advances in Organic Geochemistry 1979* (eds. A. G. Douglas and J. R. Maxwell). Pergamon Press, Oxford, pp. 211–217.

Duplessy J. C., Labeyrie L., Juilletleclerc A., Maitre F., Duprat J. and Sarnthein M. (1991) Surface salinity reconstruction of the North-Atlantic ocean during the last glacial maximum. *Oceanol. Acta* **14**, 311–324.

Fritz S. C., Juggins S., Battarbee R. W. and Engstrom D. R. (1991) Reconstruction of past changes in salinity and climate using a diatom-based transfer function. *Nature* **352**, 706.

Fröhlich K., Grabczak J. and Rozankski K. (1988) Deuterium and Oxygen-18 in the Baltic Sea. *Chem. Geol.* **72**, 77–83.

Garcia, H. E., Locarnini, R. A., Boyer, T. P., Antonov, J. I., Zweng, M. M., Baranova, O. K., Johnson, D. R. (2010) World Ocean Atlas 2009, vol. 4, Nutrients (Phosphate, Nitrate, Silicate), NOAA Atlas NESDIS, vol. 71. US Gov. Print. Off., Washington, DC.

Gould J., Kienast M., Dowd M. and Schefuß E. (2019) An open-ocean assessment of alkenone δD as a paleo-salinity proxy. *Geochim. Cosmochim. Ac.* **246**, 478–497.

Häggi C., Chiessi C. M. and Schefuß E. (2015) Testing the D/H ratio of alkenones and palmitic acid as salinity proxies in the Amazon Plume. *Biogeosciences* **12**, 7239–7249.

Kaiser J., van der Meer M. T. and Arz H. W. (2017) Long-chain alkenones in Baltic Sea surface sediments: new insights. *Org. Geochem.* **112**, 93–104.

Kaiser J., Wang K. J., Rott D., Li G., Zheng Y., Amaral-Zettler L., Arz H. W. and Huang Y. (2019) Changes in long chain alkenone distributions and Isochrysidales groups along the Baltic Sea salinity gradient. *Org. Geochem.* **127**, 92–103.

Kasper S., van der Meer M. T. J., Mets A., Zahn R., Sinninghe Damsté J. S. and Schouten S. (2014) Salinity changes in the Agulhas leakage area recorded by stable hydrogen isotopes of C_{37} alkenones during Termination I and II. *Clim. Past* **10**, 251–260.

Kasper S., van der Meer M. T., Castañeda I. S., Tjallingii R., Brummer G. J. A., Damsté J. S. S. and Schouten S. (2015) Testing the alkenone D/H ratio as a paleo indicator of sea surface salinity in a coastal ocean margin (Mozambique Channel). *Org. Geochem.* **78**, 62–68.

Knappertsbusch M. (1993) Geographic distribution of living and Holocene coccolithophores in the Mediterranean Sea. *Mar. Micropaleontol.* **21**, 219–247.

Leduc G., Sachs J. P., Kawka O. E. and Schneider R. R. (2013) Holocene changes in eastern equatorial Atlantic salinity as estimated by water isotopologues. *Earth Planet Sc. Lett.* **362**, 151–162.

Locarnini R. A., Mishonov A. V., Antonov J. I., Boyer T. P. and Garcia H. E. (2010) World Ocean Atlas 2009, Volume 2: Salinity. In *NOAA Atlas NESDIS 69* (ed. S. Levitus). U.S. Government Printing Office, Washington, D.C., p. 184.

Lochte K., Ducklow H. W., Fasham M. J. R. and Stienens C. (1993) Plankton succession and carbon cycling at 47° N, 20° W during the JGOFS North Atlantic bloom experiment. *Deep-Sea Res.* **40**, 91–114.

Lomas M. W. and Bates N. R. (2004) Potential controls on interannual partitioning of organic carbon during the winter/spring phytoplankton bloom at the Bermuda Atlantic Time-series Study (BATS) site. *Deep-Sea Res. Pt. I* **51**, 1619–1636.

Longo W. M., Dillon J. T., Tarozo R., Salacup J. M. and Huang Y. (2013) Unprecedented separation of long chain alkenones from gas chromatography with a poly(trifluoropropylmethlsiloxane) stationary phase. *Org. Geochem.* **65**, 94–102.

M'Boule D., Chivall D., Sinke-Schoen D., Sinninghe Damsté J. S., Schouten S. and van der Meer M. T. J. (2014) Salinity dependent hydrogen isotope fractionation in alkenones produced by coastal and open ocean haptophyte algae. *Geochim. Cosmochim. Ac.* **130**, 126–135.

McIntyre A. and Bé A. W. (1967) Modern coccolithophoridae of the Atlantic Ocean—I. Placoliths and cyrtoliths. *Deep-Sea Res.* **14**, 561–597.

Moncheva S., Gotsis-Skretas O., Pagou K. and Krastev A. (2001) Phytoplankton blooms in Black Sea and Mediterranean coastal ecosystems subjected to anthropogenic eutrophication: similarities and differences. *Estuar. Coast. Shelf S.* **53**, 281–295.

Müller P. J., Kirst G., Ruhland G., Von Storch I. and Rosell-Melé A. (1998) Calibration of the alkenone paleotemperature index U 37 K′ based on core-tops from the eastern South Atlantic and the global ocean (60° N-60° S). *Geochim. Cosmochim. Ac.* **62**, 1757–1772.

Nelson D. B. and Sachs J. P. (2014) The influence of salinity on D/H fractionation in alkenones from saline and hypersaline lakes in continental North America. *Org. Geochem.* **66**, 38–47.

Ohkouchi N., Eglinton T. I., Keigwin L. D. and Hayes J. M. (2002) Spatial and temporal offsets between proxy records in a sediment drift. *Science* **298**, 1224–1227.

Pahnke K., Sachs J. P., Keigwin L., Timmermann A. and Xie S. P. (2007) Eastern tropical Pacific hydrologic changes during the past 27,000 years from D/H ratios in alkenones. *Paleoceanography* **22**, 1–15.

Petrick B. F., McClymont E. L., Marret F. and Meer M. T. (2015) Changing surface water conditions for the last 500 ka in the Southeast Atlantic: implications for variable influences of Agulhas leakage and Benguela upwelling. *Paleoceanography* **30**, 1153–1167.

Prahl F. G., Popp B. N., Karl D. M. and Sparrow M. A. (2005) Ecology and biogeochemistry of alkenone production at Station ALOHA. *Deep Sea Res. Part 1* **52**, 699–719.

Rohling E. J. (2000) Paleosalinity: confidence limits and future applications. *Mar. Geol.* **163**, 1–11.

Rohling E. J. (2007) Progress in paleosalinity: overview and presentation of a new approach. *Paleoceanography* **22**.

Sachs J. P. and Kawka O. E. (2015) The influence of growth rate on $^2H/^1H$ fractionation in continuous cultures of the coccolithophorid *Emiliania huxleyi* and the diatom *Thalassiosira pseudonana*. *PLoS One* **10**.

Sachs J. P., Maloney A. P., Gregersen J. and Paschall C. (2016) Effect of salinity on $^2H/^1H$ fractionation in lipids from continuous cultures of the coccolithophorid *Emiliania huxleyi*. *Geochim. Cosmochim. Ac.* **189**, 96–109.

Sachse D., Billault I., Bowen G. J., Chikaraishi Y., Dawson T. E., Feakins S. J., Freeman K. H., Magill C. R., McInerney F. A., van der Meer M. T. J., Polissar P., Robins R. J., Sachs J. P., Schmidt A., Sessions A. L., White J. W. C., West J. B. and Kahmen A. (2012) Molecular paleohydrology: interpreting the hydrogen-isotopic composition of lipid biomarkers from photosynthesizing organisms. *Annu. Rev. Earth Planet Sci.* **40**, 221–249.

Schmidt G. A., Bigg G. R. and Rohling, E. J. (1999) Global Seawater Oxygen-18 Database - v1.22. <https://data.giss.nasa.gov/o18data/>.

Schouten S., Ossebar J., Shreiber K., Kienhuis M. V. M., Benthien A. and Bijma J. (2006) The effect of temperature, salinity and growth rate on the stable hydrogen isotopic composition of long chain alkenones produced by *Emiliania huxleyi* and *Gephyrocapsa oceanica*. *Biogeosciences* **3**, 113–119.

Schulz H. M., Schöner A. and Emeis K. C. (2000) Long-chain alkenone patterns in the Baltic Sea – an ocean-freshwater transition. *Geochim. Cosmochim. Ac.* **64**, 469–477.

Schwab V. F. and Sachs J. P. (2011) Hydrogen isotopes in individual alkenones from the Chesapeake Bay estuary. *Geochim. Cosmochim. Ac.* **75**, 7552–7565.

Simon M. H., Gong X., Hall I. R., Ziegler M., Barker S., Knorr G., Meer M. T., Kasper S. and Schouten S. (2015) Salt exchange in the Indian Atlantic Ocean Gateway since the Last Glacial Maximum: a compensating effect between Agulhas Current changes and salinity variations? *Paleoceanography* **30**, 1318–1327.

Tierney J. E. and Tingley M. P. (2018) BAYSPLINE: a new calibration for the alkenone paleothermometer. *Paleoceanography* **33**, 281–301.

Tyrrell T., Schneider B., Charalampopoulou A. and Riebesell U. (2008) Coccolithophores and calcite saturation state in the Baltic and Black Seas. *Biogeosciences* **5**, 485–494.

van der Meer M. T., Baas M., Rijpstra W. I. C., Marino G., Rohling E. J., Damsté J. S. S. and Schouten S. (2007) Hydrogen isotopic compositions of long-chain alkenones record freshwater flooding of the Eastern Mediterranean at the onset of sapropel deposition. *Earth Planet Sc. Lett.* **262**, 594–600.

van der Meer M. T. J., Benthein A., Bijma J., Schouten S. and Sinninghe Damste J. S. (2013) Alkenone distribution impacts the hydrogen isotopic composition of the $C_{37:2}$ and $C_{37:3}$ alkan-2-ones in Emiliania huxleyi. *Geochim. Cosmochim. Ac.* **111**, 162–166.

van der Meer M. T. J., Benthien A., French K. L., Epping E., Zondervan I., Reichart G. J., Bijma J., Sinninghe Damsté J. S. and Schouten S. (2015) Large effect of irradiance on hydrogen isotope fractionation of alkenones in *Emiliania huxleyi*. *Geochim. Cosmochim. Ac.* **160**, 16–24.

Vepsäläinen J., Pyhälahti T., Rantajärvi E., Kallio K., Pertola S., Stipa T., Kiirikki M., Pulliainen J. and Seppälä J. (2005) The combined use of optical remote sensing data and unattended flow-through fluorometer measurements in the Baltic Sea. *Int. J. Rem. Sens.* **26**, 261–282.

Volkman J. K., Eglinton G., Corner E. D. S. and Sargent J. R. (1980) Novel unsaturated straight-chain C37–C39 methyl and ethyl ketones in marine sediments and a coccolithophore *Emiliania huxleyi*. *Phys. Chem. Earth* **12**, 219–227.

Wall D. and Dale B. (1968) Modern dinoflagellate cysts and evolution of the Peridiniales. *Micropaleontology* **14**, 265–304.

Warden L., van der Meer M. T. J., Moros M. and Sinninghe Damsté J. S. (2016) Sedimentary alkenone distributions reflect salinity changes in the Baltic Sea over the Holocene. *Org. Geochem.* **102**, 30–44.

Weiss G. M., Pfannerstill E. Y., Schouten S., Damsté J. S. S. and van der Meer M. T. J. (2017) Effects of alkalinity and salinity at low and high light intensity on hydrogen isotope fractionation of long-chain alkenones produced by *Emiliania huxleyi*. *Biogeosciences* **14**, 5693–5704.

Wilson S. E., Cumming B. F. and Smol J. P. (1994) Diatom-salinity relationships in 111 lakes from the Interior Plateau of British Columbia, Canada: the development of diatom-based models for paleosalinity reconstructions. *J. Paleolimnol.* **12**, 197–221.

Wolfshorndl M., Danford R. and Sachs J. P. (2019) 2H/1H fractionation in microalgal lipids from the North Pacific Ocean: growth rate and irradiance effects. *Geochim. Cosmochim. Ac.* **246**, 317–338.

Wolhowe M. D., Prahl F. G., Probert I. and Maldonado M. (2009) Growth phase dependent hydrogen isotopic fractionation in alkenone-producing haptophytes. *Biogeosciences* **6**, 1681–1694.

Wolhowe M. D., Prahl F. G., Langer G., Oviedo A. M. and Ziveri P. (2015) Alkenone δD as an ecological indicator: a culture and field study of physiologically-controlled chemical and hydrogen-isotopic variation in C_{37} alkenones. *Geochim. Cosmochim. Ac.* **162**, 166–182.

Xu L., Reddy C. M., Farrington J. W., Frysinger G. S., Gaines R. B., Johnson C. G., Nelson R. K. and Eglinton T. I. (2001) Identification of a novel alkenone in Black Sea sediments. *Org. Geochem.* **32**, 633–646.

Ziveri P., Rutten A., De Lange G. J., Thomson J. and Corselli C. (2000) Present-day coccolith fluxes recorded in central eastern Mediterranean sediment traps and surface sediments. *Palaeogeogr. Palaeocl.* **158**, 175–195.

Associate editor: Jessica Tierney